Overview of Model Predictive Control for Induction Motor Drives

Yongchang Zhang[1]*, *Bo Xia*[1], *Haitao Yang*[1], and *Jose Rodriguez*[2]

(1. Inverter Technologies Engineering Research Center of Beijing,
North China University of Technology, Beijing, 100144, China
2. Universidad Andres Bello, Santiago, Chile.)

Abstract: Model predictive control (MPC) has attracted widespread attention in both academic and industry communities due to its merits of intuitive concept, quick dynamic response, multi-variable control, ability to handle various nonlinear constraints, and so on. It is considered a powerful alternative to field oriented control (FOC) and direct torque control (DTC) in high performance AC motor drives. Compared to FOC, MPC eliminates the use of internal current control loops and modulation block, hence featuring very quick dynamic response. Compared to DTC, MPC uses a cost function rather than a heuristic switching table to select the best voltage vector, producing better steady state performance. In spite of the merits above, MPC also presents some drawbacks such as high computational burden, nontrivial weighting factor tuning, high sampling frequency, variable switching frequency, model/parameter dependence and relatively high steady ripples in torque and stator flux. This paper presents the state of the art of MPC in high performance induction motor (IM) drives, and in particular the progress on solving the drawbacks of conventional MPC. Finally, one of the improved MPC is compared to FOC to validate its superiority. It is shown that the improved MPC has great potential in the future high performance AC motor drives.

Keywords: Model predictive control (MPC), field oriented control(FOC), direct torque control (DTC), induction motor (IM).

1 Introduction

For decades, FOC and DTC have been the two most popular and mature control methods for high performance control of AC motor drives[1]. In FOC, the stator currents are decomposed into d-axis (corresponding to flux) component and q-axis (corresponding to torque) component to emulate the behavior of a DC machine, where the d-axis is in alignment with the position of rotor flux vector. As a result, decoupled control of torque and rotor flux is achieved. Both d-axis and q-axis currents are regulated in the synchronous frame using two proportional-integral(PI) controllers. A space vector modulation(SVM) block is subsequently used to synthesize the reference voltage vector, generating the final gating pulses for the inverters. Good steady state performance and quick dynamic response are achieved in FOC and it has become the industrial standard for high performance drives[2].

DTC was proposed firstly in the area of induction motor drives[3-4], and later extended to other kinds of three-phase AC machines and converters[5-6]. Compared to FOC, DTC eliminates the use of current control and SVM block. It directly selects the most appropriate voltage vector from a predefined switching table according to the position of stator flux and error signs of torque and stator flux. Very quick dynamic response is achieved in DTC with simple structure. The main drawbacks of DTC are high torque ripples in steady state and variable switching frequency[7]. Furthermore, low speed operation is usually an issue of DTC[8]. Various methods have been proposed to tackle the problems above by using SVM[9], duty cycle control[10]and multilevel converter[11], etc. However, they generally increase the computational burden and/or hardware cost.

With the development of electronics technology and information technology, more powerful digital signal processors (DSP) and microprocessors are available at reduced cost. As a result, very sophisticated and advanced modern control theory can be applied to AC motor drives. Among various modern control theories, MPC is one of the most outstanding control methods due to its merits of intuitive concept, quick dynamic response, multi-variable control, ability to handle various nonlinear constraints, and so on. For high performance induction motor drives, usually torque and stator flux are selected as the control variables. In conventional MPC, a cost function relating to torque and flux errors is defined and evaluated for each voltage vector and the one minimizing the cost function is selected as the best voltage vector[12]. Although the vector selected from MPC is more accurate and effective than the one selected from a predefined switching table in DTC, the steady state performance is still not satisfactory and inferior to that of FOC[13]. The main reason is that only one voltage vector is applied during one control period, which cannot regulate the torque and stator flux accurately and moderately[14]. The enumeration-based prediction requires lots of calculations and is computational intensive. The sampling frequency has

* Corresponding Author, E-mail: zyc@ncut.edu.cn.

to be high, usually tens of kilohertz but the switching frequency is variable. Furthermore, as torque and stator flux are different in amplitude and units, a proper weighting factor must be designed in the cost function, which is not an easy task due to the lack of theoretical guidance[15]. Finally, MPC relies on the accuracy of system model and machine parameters, which may affect its performance if there is mismatch in the machine parameters. To make MPC practical, additional issue such as starting current limitation, and sensor-less operation, should also be considered.

To overcome the drawbacks of conventional MPC, various improved MPC have been proposed in the literature. This paper presents an overview of state of the art of MPC in high performance torque control of induction motor drives. A brief review of the basic principle of conventional MPC is introduced in Section 2. The issue of weighting factor tuning is given in Section 3. The issue of control complexity reduction is shown in Section 4. In Section 5, the steady state performance of conventional MPC is significantly improved by introducing two or three vectors during one control period. The practical issue of sensor-less operation of MPC is introduced in Section 6. A comparison of FOC and an improved MPC is introduced in Section 7 to show the potential of MPC in induction motor drives. Finally, some conclusions are given in Section 8. This paper will help to understand the advantages and challenges of MPC when applied to high performance induction motor drives.

2 Basic principle of MPC

2.1 Dynamic model of IM

A mathematical model of an induction motor described by space vectors in an arbitrary frame rotating at ω_k speed is expressed as:

Voltage equations:

$$\begin{cases} \boldsymbol{u}_s = R_s \boldsymbol{i}_s + p\boldsymbol{\psi}_s + \mathrm{j}\omega_k \boldsymbol{\psi}_s \\ 0 = R_r \boldsymbol{i}_r + p\boldsymbol{\psi}_r + \mathrm{j}(\omega_k - \omega_r)\boldsymbol{\psi}_r \end{cases} \tag{1}$$

Flux equation:

$$\begin{cases} \boldsymbol{\psi}_s = L_s \boldsymbol{i}_s + L_m \boldsymbol{i}_r \\ \boldsymbol{\psi}_r = L_m \boldsymbol{i}_s + L_r \boldsymbol{i}_r \end{cases} \tag{2}$$

Torque equation:

$$T_e = \frac{3}{2} N_p \boldsymbol{\psi}_s \otimes \boldsymbol{i}_s = \frac{3}{2} N_p \lambda L_m \boldsymbol{\psi}_r \otimes \boldsymbol{\psi}_s \tag{3}$$

where $p = \mathrm{d}/\mathrm{d}t$ is the operator of differentiation; $\boldsymbol{u}_s$,$\boldsymbol{i}_s$, $\boldsymbol{i}_r$, $\boldsymbol{\psi}_s$ and $\boldsymbol{\psi}_r$ are the stator voltage, stator current, rotor current, stator flux linkage and rotor flux linkage vector, respectively; R_s, R_r, L_s, L_r and L_m are the stator resistance, rotor resistance, stator inductance, rotor inductance and mutual inductance, respectively; ω_r and N_p are the electrical rotor speed and pole pairs and $\lambda=1/(L_s L_r - L_m^2)$.

In stationary frame (ω_k=0), the state space model of IM can be rearranged by using state space equations[16-18] as:

$$p\boldsymbol{x} = \boldsymbol{A}\boldsymbol{x} + \boldsymbol{B}\boldsymbol{u} \tag{4}$$

where $\boldsymbol{x} = \begin{bmatrix} \boldsymbol{i}_s & \boldsymbol{\psi}_s \end{bmatrix}^{\mathrm{T}}$ are the state variable vector and

$$\boldsymbol{A} = \begin{bmatrix} -\lambda(R_s L_r + R_r L_s) + \mathrm{j}\omega_r & \lambda(R_r - \mathrm{j}L_r\omega_r) \\ -R_s & 0 \end{bmatrix}$$

$$\boldsymbol{B} = \begin{bmatrix} \lambda L_r \\ 1 \end{bmatrix}$$

In digital implementation, the equation (4) must be discretized to predict torque and flux at (k+1)th instant for a given voltage vector. A simple way to discretize (4) is using first-order Euler method. However, its accuracy is relatively limited especially during high speed operation[19]. In [18], an improved discrete model of IM is obtained by using the Cayley–Hamilton theorem to compute the matrix exponential, which is quite complicated. To achieve higher accuracy and avoid complicated calculation, the Heun's method[20] is employed in this paper, which is expressed as:

$$\begin{cases} \boldsymbol{x}_p^{k+1} = \boldsymbol{x}^k + T_{sc}(\boldsymbol{A}\boldsymbol{x}^k + \boldsymbol{B}\boldsymbol{u}_s^k) \\ \boldsymbol{x}^{k+1} = \boldsymbol{x}_p^{k+1} + \dfrac{T_{sc}}{2}\boldsymbol{A}(\boldsymbol{x}_p^{k+1} - \boldsymbol{x}^k) \end{cases} \tag{5}$$

where T_{sc} is control period; $\boldsymbol{x}_p^{k+1}$ is predictor-correctors of state vector; $\boldsymbol{x}^{k+1}$ is predicted state vector of stator current and stator flux at (k+1)th instant.

The rotor flux at (k+1)th instant can be estimated by stator flux $\boldsymbol{\psi}_s^{k+1}$ and current $\boldsymbol{i}_s^{k+1}$ as:

$$\boldsymbol{\psi}_r^{k+1} = \frac{L_r}{L_m}\boldsymbol{\psi}_s^{k+1} - \frac{1}{\lambda L_m}\boldsymbol{i}_s^{k+1} \tag{6}$$

Consequently, the electromagnetic torque can be predicted as:

$$T_e = \frac{3}{2} N_p \lambda L_m \boldsymbol{\psi}_r^{k+1} \otimes \boldsymbol{\psi}_s^{k+1} \tag{7}$$

where $\otimes$ represents cross product of two vectors.

2.2 State estimation

Accurate state estimation of state variable is a key factor for ensuring a good performance of MPC in real-time implementation. A full order observer for the flux and torque estimation is adopted due to its accuracy and insensitivity to parameter variation over a wide speed range. The mathematical model of the observer is shown as follows:

$$\frac{\mathrm{d}\hat{\boldsymbol{x}}}{\mathrm{d}t} = A\hat{\boldsymbol{x}} + B\boldsymbol{u} + G(\boldsymbol{i}_s - \hat{\boldsymbol{i}}_s) \tag{8}$$

where $\hat{\boldsymbol{x}} = \begin{bmatrix} \hat{\boldsymbol{i}}_s & \hat{\boldsymbol{\psi}}_s \end{bmatrix}^{\mathrm{T}}$ are the estimated state for stator current and stator flux.

A constant gain matrix G is employed in this paper to improve the stability of the observer and is expressed as:

$$G = -\begin{bmatrix} 2b \\ b/(\lambda L_r) \end{bmatrix} \tag{9}$$

where b is a negative constant gain. This gain matrix can improve the convergence and stability of observer, especially at high speed as shown in [8]. In this paper, b is chosen as −40. The characteristic of the observer can be found in [21], which presents a strong robustness over a wide speed range.

To illustrate the influence of machine parameter variations on the performance of the system, Fig.1 shows the simulated response of MPC at low and high speeds, when the stator and rotor resistance are increased by 50% and 100%, respectively. It is seen that the system works well at both low and high speeds, even if the stator and rotor resistances vary significantly from their actual value. The current is very sinusoidal in shape. The simulation results prove that the proposed gain matrix has a strong tolerance for machine parameter variation.

2.3 Vector selection

Recently, MPC has been introduced as a powerful control method for IM drives. The control diagram of MPC is shown in Fig.2. In model predictive torque

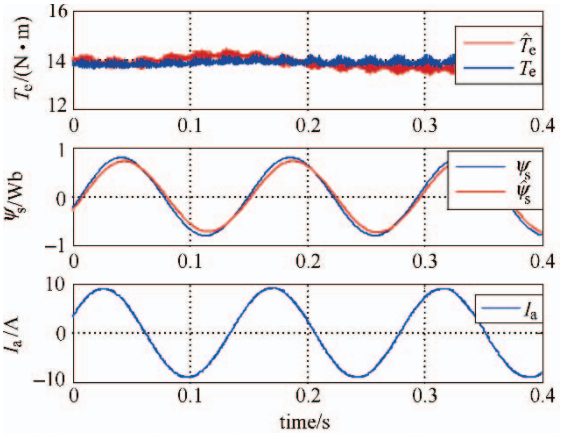

(a) both the stator and rotor resistances are increased by 50% at 150r/min

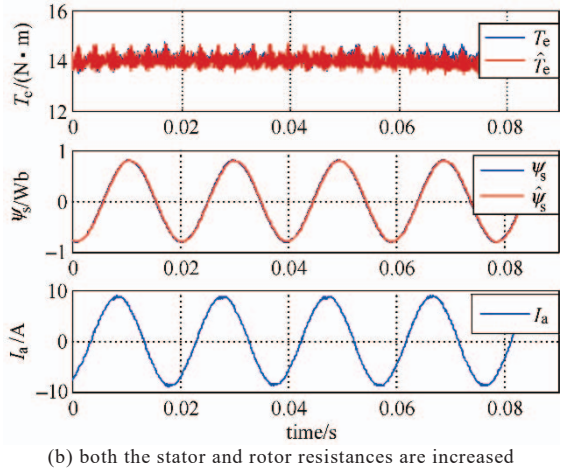

(b) both the stator and rotor resistances are increased by 100% at 1500 r/min

Fig.1 Simulated responses of MPC with mismatched machine parameters

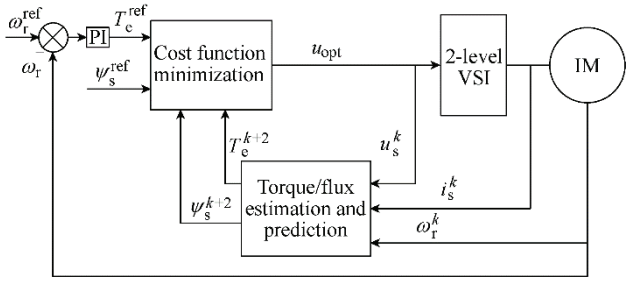

Fig.2 Control diagram of MPTC

control (MPTC), the cost function is usually defined as the linear combination of torque and flux errors to determine the best voltage vector, which is expressed as [14,22]:

$$G = |T_e^{ref} - T_e^{k+1}| + k_\psi \|\boldsymbol{\psi}_s^{ref}| - |\boldsymbol{\psi}_s^{k+1}\| \tag{10}$$

where k_ψ is a weighting factor for stator flux.

In digital implementation, there is usually one-step delay between applied voltage vector and the selected vector. To eliminate the side effect caused by one-step delay, a model-based two-step prediction is usually employed[16]. Thus, by considering one-step delay in practical application, the following cost function should be evaluated to select the best voltage vector.

$$G_1 = |T_e^{ref} - T_e^{k+2}| + k_\psi \|\boldsymbol{\psi}_s^{ref}| - |\boldsymbol{\psi}_s^{k+2}\| \tag{11}$$

It should be noted that the torque reference is generated from an outer speed loop and it is usually assumed constant from the k to k+2 instant, because the time constant of mechanical speed is much larger than that of torque. In fact, this assumption is a common practice in most study regarding MPTC as shown in [23-29].

For a two-level inverter-fed IM drive system, there are eight switching states and seven different voltage vectors, $u_{0(7)}$,u_1,u_2…u_6 as shown in Fig.3. For each voltage vector, the cost function value of MPTC may be different. After the cost function G_1 is evaluated for each value, the vector producing minimal G_1 is selected as the best one.

3 Control complexity reduction

As is well known, the implementation of MPTC requires a high sampling frequency to obtain a good performance in the real-time implementation because

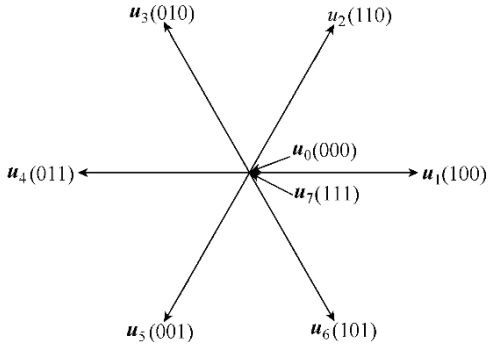

Fig.3 Voltages vectors and corresponding switching states of the two level inverter

only one voltage vector is applied in whole control period. Hence, reducing the control complexity for MPTC has become an important topic[30].

In MPTC，both stator current and stator flux have to be predicted for seven instances to obtain the estimated torque from (7) for each voltage vector, which is time consuming and computational intensive. As stator current is not directly needed when evaluating the cost function in (11), the prediction of stator current may be eliminated for control complexity reduction. The remaining stator flux prediction is very simple, as shown in the second row of equation (4).

From (4), the equation of stator current is obtained as:

$$\frac{\mathrm{d}\boldsymbol{i}_\mathrm{s}}{\mathrm{d}t}=[-\lambda(R_\mathrm{s}L_\mathrm{r}+R_\mathrm{r}L_\mathrm{s})+\mathrm{j}\omega_\mathrm{r}]\boldsymbol{i}_\mathrm{s}+\lambda(R_\mathrm{r}-\mathrm{j}L_\mathrm{r}\omega_\mathrm{r})\boldsymbol{\psi}_\mathrm{s}+\boldsymbol{u}_\mathrm{s} \tag{12}$$

Substitute (1) into (12) and eliminate $\boldsymbol{u}_\mathrm{s}$, the current at ($k$+1)th instant can be obtained from equation (12) by using forward Euler discretization method[31] as:

$$\boldsymbol{i}_\mathrm{s}(k+1)=\boldsymbol{i}_{\mathrm{s}0}(k)+\lambda L_\mathrm{r}\boldsymbol{\psi}_\mathrm{s}(k+1) \tag{13}$$

$$\boldsymbol{i}_{\mathrm{s}0}(k)=(1-\lambda R_\mathrm{r}L_\mathrm{s}T_\mathrm{sc})\boldsymbol{i}_\mathrm{s}(k)+\lambda(R_\mathrm{r}T_\mathrm{sc}-L_\mathrm{r})\boldsymbol{\psi}_\mathrm{s}(k)+\mathrm{j}\omega_\mathrm{r}T_\mathrm{sc}[\boldsymbol{i}_\mathrm{s}(k)-\lambda L_\mathrm{r}\boldsymbol{\psi}_\mathrm{s}(k)] \tag{14}$$

Substitute (13) into (7), the torque at (k+1)th instant can be simplified[31] as:

$$T_\mathrm{e}(k+1)=\frac{3N_\mathrm{p}}{2}\boldsymbol{\psi}_\mathrm{s}^{k+1}\otimes\boldsymbol{i}_{\mathrm{s}0}(k) \tag{15}$$

because $\boldsymbol{\psi}_\mathrm{s}^{k+1}\otimes\boldsymbol{\psi}_\mathrm{s}^{k+1}=0$.

The main advantage of using equation (15) to calculate torque is that only $\boldsymbol{\psi}_\mathrm{s}^{k+1}$ has to be predicted seven times for different voltage vectors, whereas $\boldsymbol{i}_{\mathrm{s}0}(k)$ is only related to the variables at the kth instant and only needed to be calculated once. As the stator flux prediction is very simple, the overall computational burden is significantly reduced.

4 Weighting factor tuning

It can be seen that the basic principle of MPTC is very simple, however, the design of weighting factor is a nontrivial work due to the absence of theoretical guidance. On one hand, if the weighting factor of stator flux in MPTC is too high, the term reflecting torque error becomes negligible. However, this only guarantees that the amplitude of stator flux is close to the reference value and may lose the control of torque. On the other hand, if the weighting factor is too small, the stator flux cannot be accurately controlled, which produces high oscillations in flux amplitude and spikes in the stator currents. Consequently, The weighting factor usually requires tedious tuning work by simulation and experimental tests to find a suitable value, which restricts the application of MPTC in practice.

4.1 Model predictive flux control

To avoid the use of weighting factor in MPTC, a new stator flux vector reference can be equivlently constructed from $T_\mathrm{e}^\mathrm{ref}$ and $\psi_\mathrm{s}^\mathrm{ref}$ based on the model of IM. As only stator flux is used, this method is called model predictive flux control (MPFC) and its control diagram is illustrated in Fig.4. The cost function of MPFC is shown in (16) and the voltage vector minimizng (16) is selected as the best vector.

$$J_1=\left|\boldsymbol{\psi}_\mathrm{s}^\mathrm{ref}-\boldsymbol{\psi}_\mathrm{s}^{k+1}\right| \tag{16}$$

Similar to MPTC, the compensation of one step delay is employed and thus the tracking error at (k+2)th instant is considered as shown in (17). It is evident that the weighting factor is no longer required as only the tracking error of stator flux vector is involved. The details of the reference conversion will be elaborated as follows.

$$J_2=\left|\boldsymbol{\psi}_\mathrm{s}^\mathrm{ref}-\boldsymbol{\psi}_\mathrm{s}^{k+2}\right| \tag{17}$$

For DTC and MPTC drives, where torque and stator flux are selected as the control variables, the stator flux reference is usually set a constant as $\psi_\mathrm{s}^\mathrm{ref}$, shown in equation (18). The main reason is that the field weakening operation and efficiency optimization are not considered in this paper, so stator flux magnitude reference is set as a constant, which is common practice in MPTC/DTC drives, as shown in [23-29]:

$$\left|\boldsymbol{\psi}_\mathrm{s}^\mathrm{ref}\right|=\psi_\mathrm{s}^\mathrm{ref} \tag{18}$$

According to (3), if rotor flux $\boldsymbol{\psi}_\mathrm{r}$ is already known, the reference value of torque and stator flux should satisfy the following equation:

$$T_\mathrm{e}^\mathrm{ref}=\frac{3}{2}N_\mathrm{p}\lambda L_\mathrm{m}(\boldsymbol{\psi}_\mathrm{r}\otimes\boldsymbol{\psi}_\mathrm{s}^\mathrm{ref}) \tag{19}$$

From (18) and (19), the stator flux vector reference $\boldsymbol{\psi}_\mathrm{s}^\mathrm{ref}$ can be expressed by $T_\mathrm{e}^\mathrm{ref}$ and $\psi_\mathrm{s}^\mathrm{ref}$ as:

$$\boldsymbol{\psi}_\mathrm{s}^\mathrm{ref}=\psi_\mathrm{s}^\mathrm{ref}\cdot\exp(\mathrm{j}\cdot\angle\boldsymbol{\psi}_\mathrm{s}^\mathrm{ref}) \tag{20}$$

$$\angle\boldsymbol{\psi}_\mathrm{s}^\mathrm{ref}=\angle\boldsymbol{\psi}_\mathrm{r}+\arcsin\left(\frac{T_\mathrm{e}^\mathrm{ref}}{\frac{3}{2}p\lambda L_\mathrm{m}\left|\boldsymbol{\psi}_\mathrm{r}\right|\psi_\mathrm{s}^\mathrm{ref}}\right) \tag{21}$$

To compensate the one-step delay, $\boldsymbol{\psi}_\mathrm{r}^{k+2}$ must be determined to obtain $\boldsymbol{\psi}_\mathrm{s}^\mathrm{ref}$ at (k+2)th instant as shown in equation (21). Consequently, the new cost function can be rebuilt as shown in equation (17).

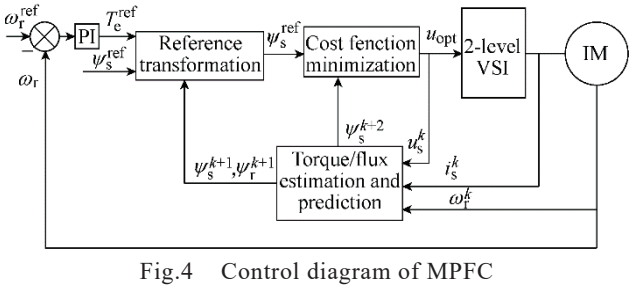

Fig.4 Control diagram of MPFC

4.2 Simulation study

Fig.5(a) shows the simulated responses of MPTC at high speed of 1500r/min when the weighting factor varies from 14.2 to 350. From top to bottom, the curves shown in Fig.5 are rotor speed, electromagnetic torque, stator flux amplitude, one phase stator current and the number of selected voltage vectors. It is seen that when the weighting factor is set to the ratio between rated torque and stator flux amplitude (k_ψ=14.2), although the torque ripples are small, there are significant oscillations in both stator flux and current. The stator flux ripples are significantly reduced when increasing k_ψ from 14.2 to 32, however, the torque ripples are also there are still spikes in the stator current. When k_ψ is increased from 32 to 100, the stator flux ripples are further reduced and the spikes in the current disappear, achieving good balance between stator flux ripples and torque ripples. Further increasing k_ψ to bigger values of 250 and 350 does not produce noticeable improvement on the flux ripples and stator current harmonics, but the torque ripples are increased, which affects the steady operation of closed-loop speed control. The results prove that k_ψ cannot be too big or too small and it must be well tuned to achieve a good steady state performance of both torque and stator flux for MPTC. For the machine in this paper, k_ψ = 100 is an appropriate solution for MPTC. On the contrary, MPFC achieves a similar steady performance to the well-tuned MPTC without the tuning of weighting factor as shown in Fig.5(b).

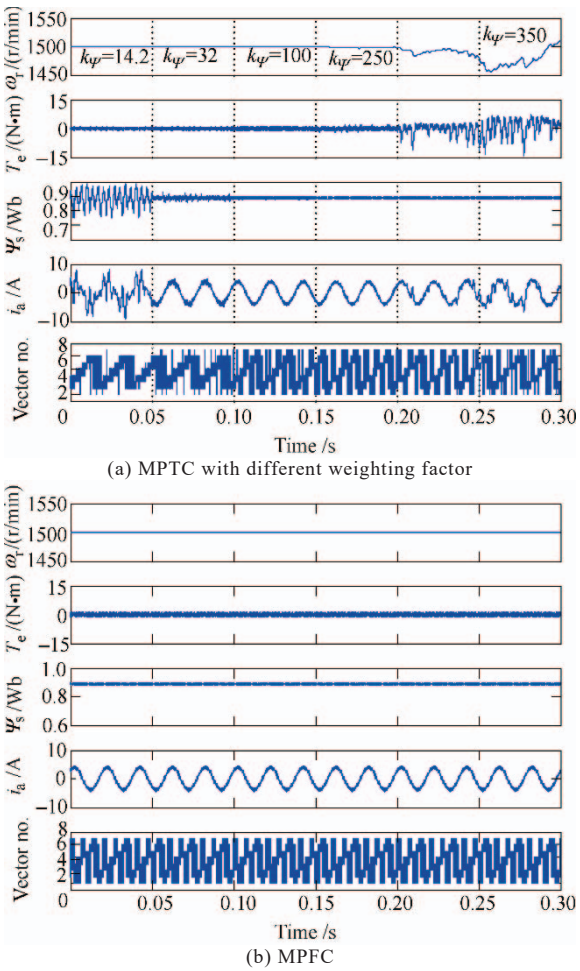

(a) MPTC with different weighting factor

(b) MPFC

Fig.5 Simulated responses at high speed operation of 1500 r/min without load for MPTC with different weighting factors and MPFC

4.3 Experimental results

Fig.6 presents the current THD for MPTC with different weighting factors and MPFC. If an improper weighting factor (e.g. k_ψ=32) is selected, the performance of MPTC degrades significantly as shown in Fig.6(a). MPFC achieves the lowest current THD, even better than that of MPTC with fine tuning weighting

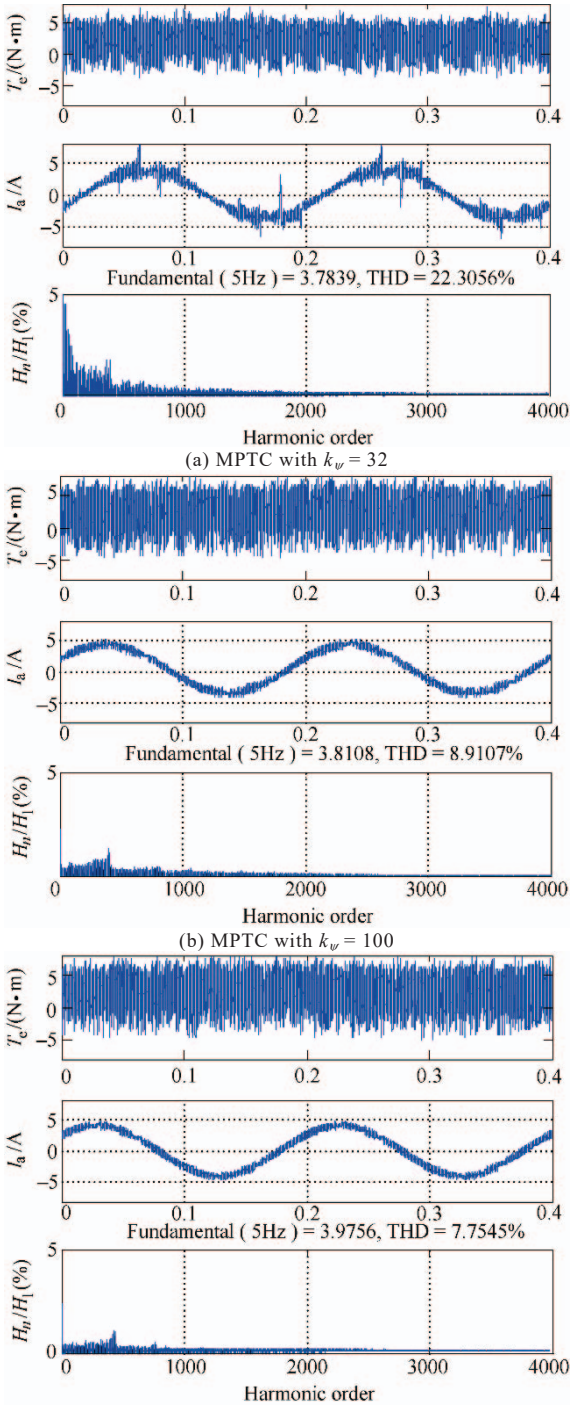

(a) MPTC with k_ψ = 32

(b) MPTC with k_ψ = 100

(c) MPFC

Fig.6 Torque and harmonic spectrum of stator current at 150 r/min without load

Factor (k_ψ=100) shown in Fig.6(b). The results indicate that a proper weighting factor has to be selected to achieve a good balance between torque ripple and stator flux ripple. By using MPFC, good balance between torque ripple and current harmonics without any tuning work can be achieved, as shown in Fig.6c. The results prove that MPTC is sensitive to the variation of weighting factor and MPFC is more practical[32].

5 Steady state performance improvement

Although MPTC is more accurate and effective than DTC in vector selection[33-35], applying the selected voltage vector during the whole control period is not optimal in terms of torque ripple reduction[36-37]. In DTC, it has been known that inserting a zero voltage vector along with an active voltage vector during one control period can achieve moderate and accurate torque regulation[38-39]. Consequently, many scholars proposed the concept of duty cycle control[40-44] by inserting a null vector along with the selected active voltage vector in MPTC and MPFC to improve their steady state performance[45].

5.1 Two-vectors-based MPTC

The active vector is first selected from conventional MPTC and then its duration is determined based on a certain principle such as deadbeat control of torque[46], torque ripple minimization[10] and mean torque control[47]. In these methods, the impact of duty ratio optimization on selecting the best voltage vector is not considered. If vector selection and duty ratio are optimized simultaneously, better steady state performance can be obtained[16]. The overall flow chart of MPTC[16] considering one-step delay compensation is shown in Fig.7.

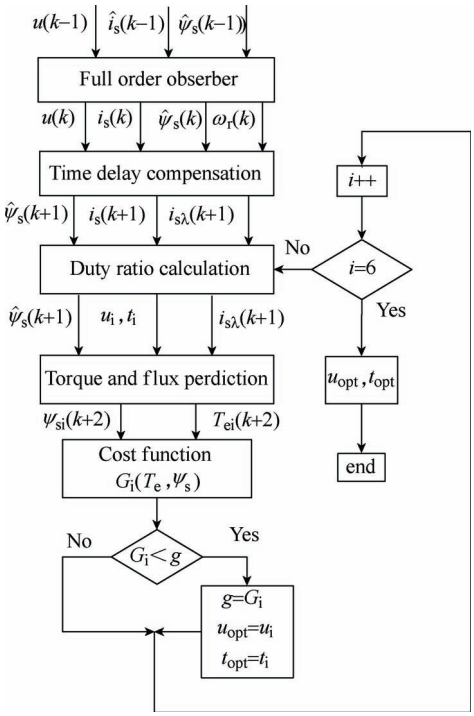

Fig.7 Flow chart of the proposed MPTC with the consideration of time-delay compensation

The MPTC[16] is experimentally tested on a two-level inverter-fed IM drive platform. The results of conventional single-vector-based MPTC[18] and the improved MPTC with separate duty cycle control[37] are also presented for the aim of comparison. For convenience, the prior method in [37] is referred as MPTC I, and MPTC[16] is referred as MPTC II in this section.

Fig.8 presents the steady-state responses at 150 r/min for conventional MPTC, MPTC I, and MPTC II. It is seen that both MPTC I and MPTC II present much lower torque ripple than that of conventional MPTC. At the same time the oscillation in stator flux

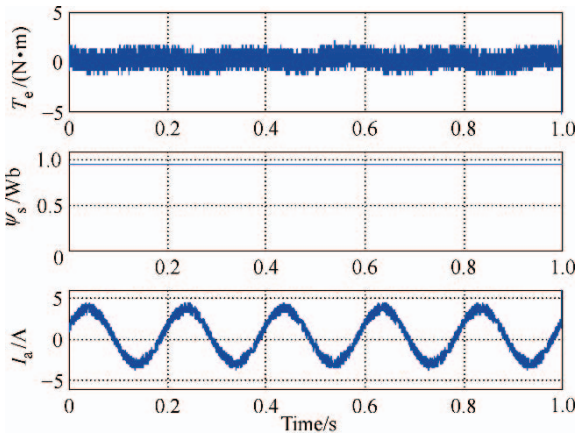

(a) Conventional MPTC at 20kHz sampling frequency

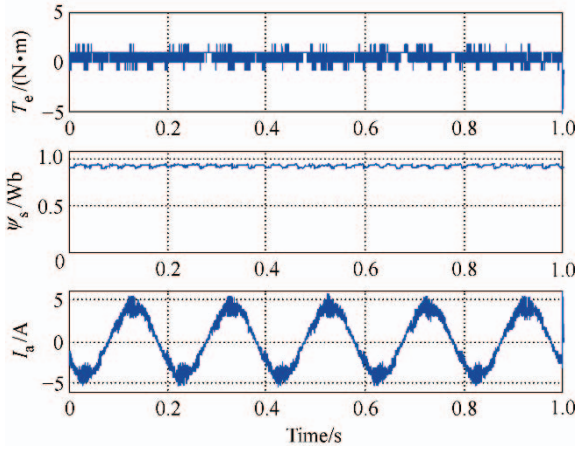

(b) MPTC I at 20kHz sampling frequency

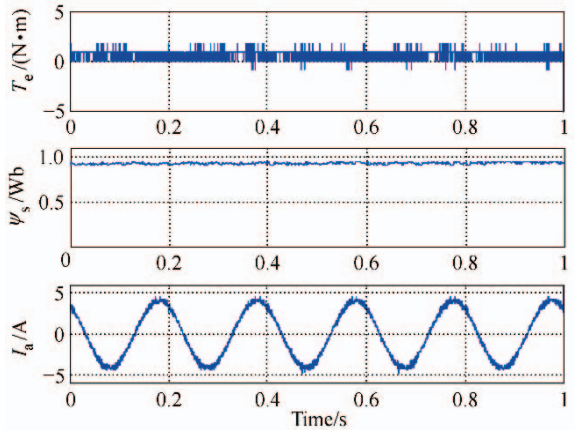

(c) MPTC II at 10kHz sampling frequency

Fig.8 Steady-state response at 150r/min for conventional MPTC, MPTC I and MPTC II

and distortion in stator current presented in MPTC I are eliminated in MPTC II, validating the effectiveness of considering the duty ratio in the cost function evaluation.

The harmonic spectrum of stator current at 150 r/min without load is shown in Fig.9. The current THD of the MPTC II is only 3.64%, much lower than the value of 8.90% in conventional MPTC. But the current THD of MPTC I is 11.16%, much higher than that of conventional MPTC and MPTC II due to the inappropriate processing of duty ratio.

The torque ripple and current THD of conventional MPTC, MPTC I, and MPTC II at various speed with rated torque are summarized in Fig.10. It is seen that

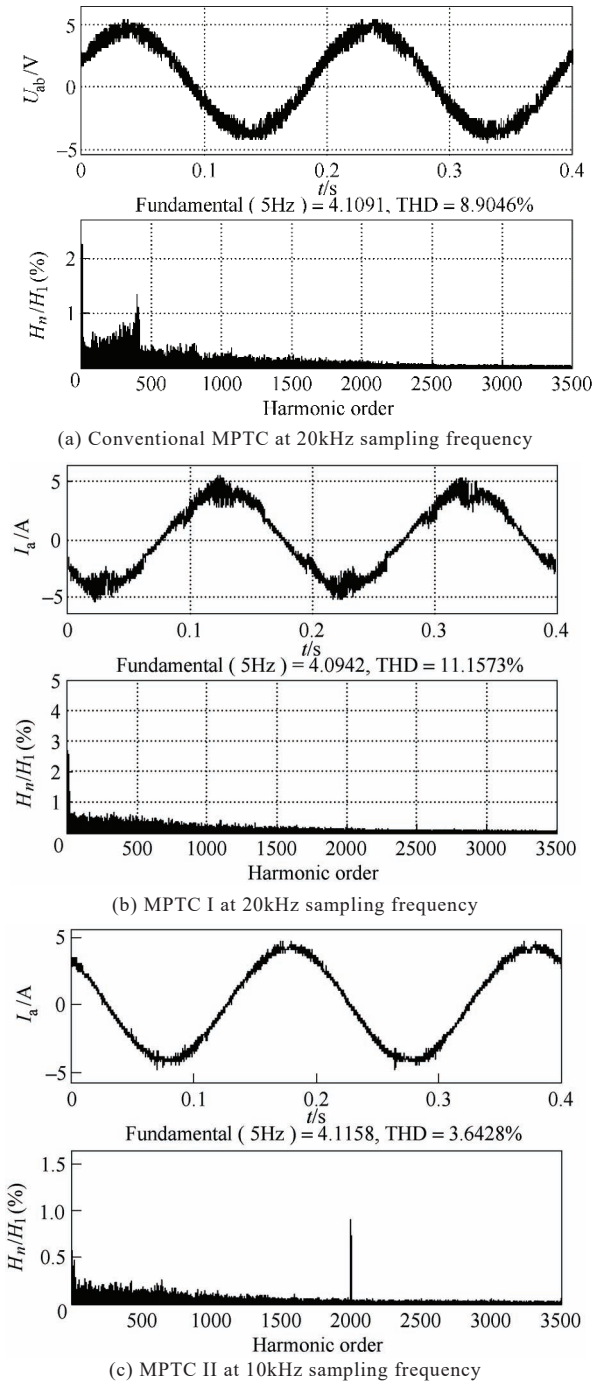

(a) Conventional MPTC at 20kHz sampling frequency

(b) MPTC I at 20kHz sampling frequency

(c) MPTC II at 10kHz sampling frequency

Fig.9 Harmonics spectrum of stator current at 150r/min for conventional MPTC, MPTC I and MPTC II

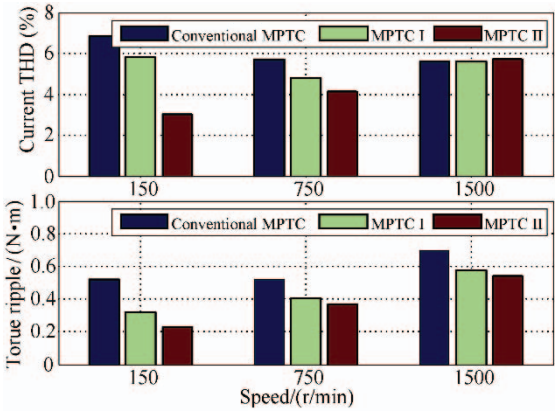

Fig.10 Torque ripple and current THD of conventional MPTC (20kHz sampling frequency), MPTC I (20kHz sampling frequency), and MPTC II (10kHz sampling frequency) at various speeds with rated load

the conventional MPTC presents the highest torque ripple at all speeds. Both MPTCI and MPTC II present much lower torque ripple, especially at low speed for MPTC II. The current THD of MPTC II is better than that of conventional MPTC and MPTC I over a wide speed range, especially at low speed. Considering the torque ripple and current THD at various speeds and the sampling frequency, the overall performance of MPTC II is the best one among the three methods.

5.2 Generalized two-vectors-based MPTC

In Section 5.1, the concept of duty cycle control was introduced in MPTC by inserting a null vector along with an active vector during one control period. However, this still fails to reduce the torque error to a minimal value due to the imposed restriction on vector combination and the cascaded processing of vector selection and vector duration. By relaxing the vector combination to two arbitrary voltage vectors, a generalized two-vectors-based MPTC (GTV-MPTC) is proposed in [14]. Experimental results were carried out to verify the effectiveness of this method. The presented results show that, compared to prior MPTC with or without duty cycle control and conventional MPTC, the GTV-MPTC achieves much better performance with lower sampling frequency over a wide speed range. For simplicity, the prior methods in [37] and[16], which use an active voltage vector and a zero vector, are named as Duty-MPTC I and Duty-MPTC II in experiment results, respectively. The conventional MPTC [18] are also presented as a comparison.

To validate that the best voltage vector combinations may not be the combination of an active vector and a null vector, Fig.11illustrates the number of selected two vectors during the startup response. The number of two null vectors are both indicated by 0 in Fig.11. It is seen that the first voltage vector is always selected as an active voltage vector, and the number of second voltage vector varies from 0 to 6. This indicates that the optimal second voltage vector is not always zero voltage vector, especially during medium and high-speed operation. Additionally, when the machine

runs at 1500 r/min, the number of selected two vectors and the corresponding pulse signal for one switch of inverter during stepped torque change is illustrated in Fig.12. It is clearly seen that the second vector may be a nonzero vector during both steady and dynamic process, confirming that relaxing the vector combinations to two arbitrary vectors in the GTV-MPTC leads to different selection of the two vectors (generally more effective) compared to Duty- MPTC II.

Fig.13 presents the responses of torque, stator flux, and stator current at 150 r/min with rated torque (14N·m). Conventional MPTC presents relatively large torque ripple, and there are many harmonics in the stator current. The torque ripple of Duty-MPTC I is lower than that of conventional MPTC, but its stator current is somewhat distorted, which is mainly caused by the cascaded processing of vector selection and vector durations. The GTV-MPTC exhibits the best steady-state performance in terms of torque and stator flux ripples as well as current harmonics among the three MPTC methods, even if its sampling frequency is only half of the other two methods.

A numerical comparison of torque ripple and THD of stator current are shown in Fig.14, which are obtained at various speeds with rated torque. It is seen that the conventional MPTC presents the highest torque ripple and current THD, followed by Duty-MPTC I. The GTV-MPTC has the lowest torque ripple and current THD at different speeds.

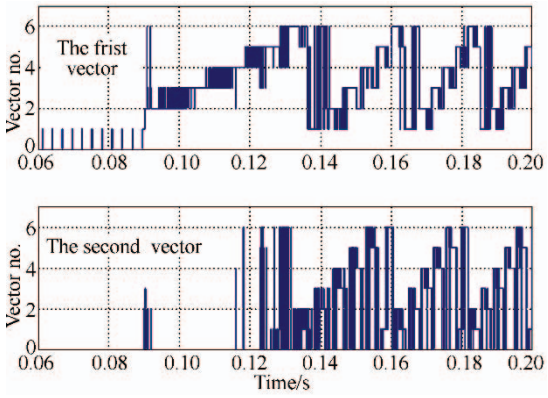

Fig.11 Selected two vectors for GTV-MPTC during startup

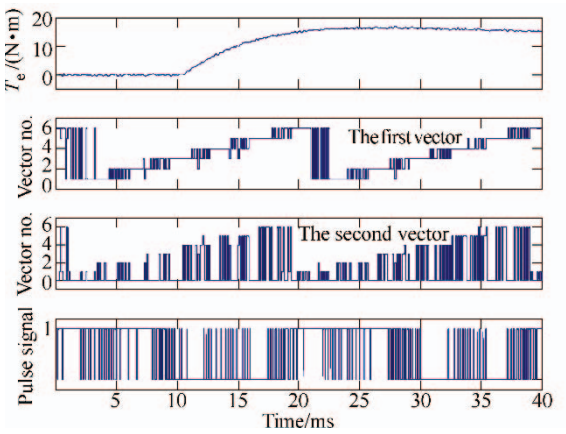

Fig.12 Selected vectors and pulse signal for GTV-MPTC during stepped load torque change

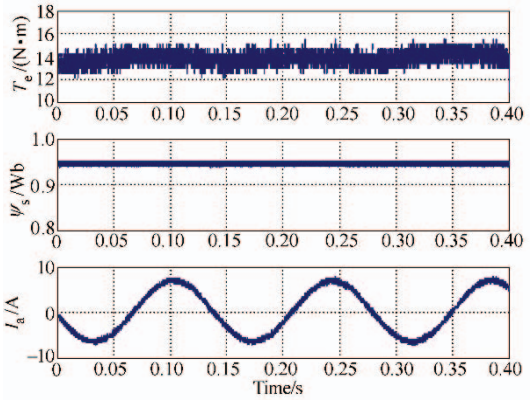

(a) Conventional MPTC

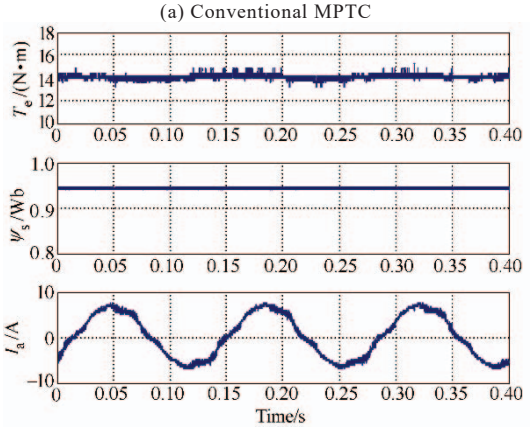

(b) Duty-MPTC I

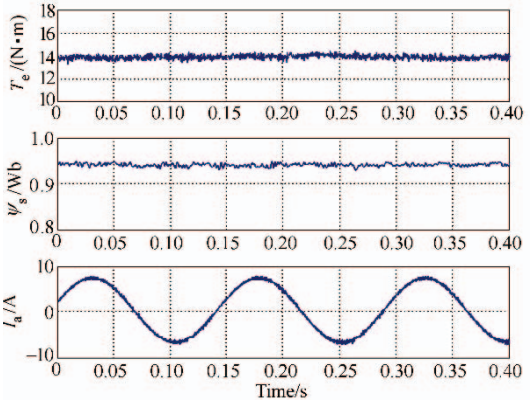

(c) GTV-MPTC

Fig.13 Low-speed operation at 150 r/min with rated torque for conventional MPTC, Duty-MPTC I, and GTV-MPTC

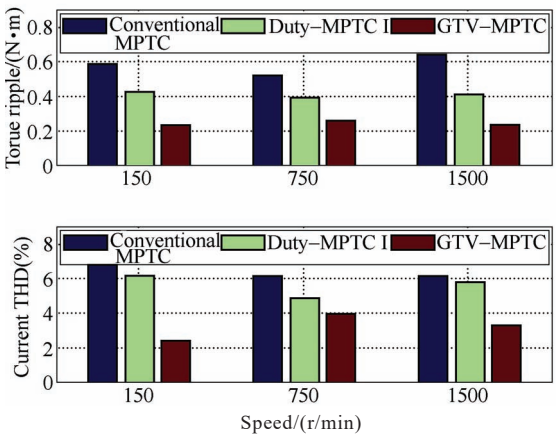

Fig.14 Comparisons of torque ripple and current THD for conventional MPTC, Duty-MPTC I, and GTV-MPTC operating at different speeds with rated load

The average switching frequency of the three methods is illustrated in Fig.15. It is clearly seen that the average switching frequency of conventional MPTC varies with speed significantly. The Duty-MPTCI presents relatively constant switching frequency, but still variable with speed, especially at high speed range. But the average switching frequency of GTV-MPTC is almost constant over a wide speed range and is even lower than that of conventional MPTC in the medium speed range. Hence, it is easy to conclude that GTV-MPTC performs best by providing the lowest torque/flux ripples and current harmonics with almost constant (and even lower) switching frequency.

A quantitative comparison between GTV-MPTC and Duty-MPTC II at various speeds is shown in Fig.16.

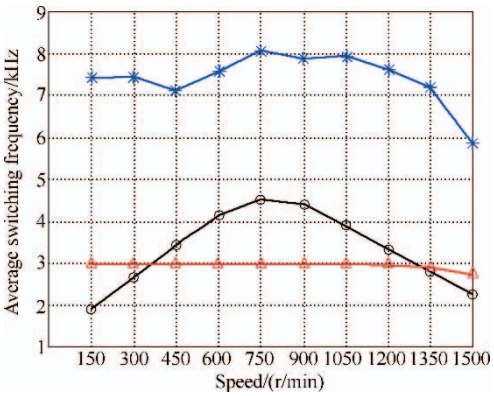

Fig.15 Average switching frequencies for conventional MPTC (marked with"o"), Duty-MPTC I (marked with "*"), and GTV-MPTC (marked with "Δ") at different speeds with rated load

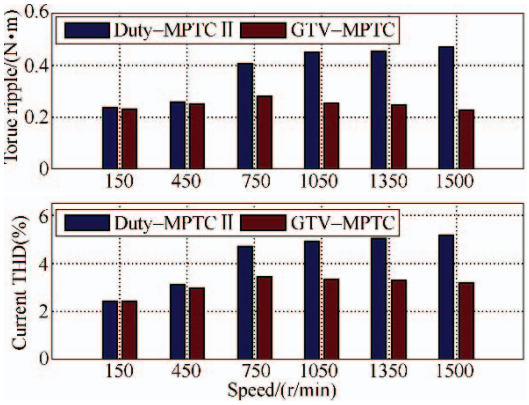

Fig.16 Comparisons of torque ripple and current THD for Duty-MPTC II and GTV-MPTC, operating at different speeds with rated load

It is seen that, the performance difference between the two methods at low speeds is minor. However, the performance of the GTV-MPTC becomes much better than Duty-MPTC II when the speed increases. This confirms that the combination of two nonzero voltage vectors are more suitable at medium and high speeds than the combination of an active vector and a null vector.

5.3 Three-vectors-based MPFC

Similar to MPTC, MPFC presents high torque and current ripples if only one voltage vector is applied during each control period. To improve the steady state performance of MPFC, various two-vectors-based schemes can be found in the existing literature. It is expected that better performance can be expected if three vectors are selected during one control period. However, the complexity would also be increased significantly, which makes its practical application difficult. To address this problem, a simple yet very effective three-vectors-based MPFC is proposed in [44], which significantly reduces the average switching frequency and computation burden.

The three-vectors-based MPFC employs two active vectors and a null vector. Similar to [45], the first voltage vector is the last voltage vector applied during the previous control period. To reduce the computational burden, the second and third vector are a zero vector and non-zero vector, respectively. The control diagram of three-vectors-based MPFC is presented in Fig.17.

The prior MPFC[45] is also presented for the aim of comparison to prove that the three-vectors-based MPFC can achieve a better performance than the two-vectors-based MPFC. For convenience, the method in [45] is refereed as method I and the three-vectors-based MPFC is refereed as method II in this section, respectively.

Fig.18 shows the dynamic responses to 100% rated load disturbance (about 14N·m) for both methods. It is seen that very similar dynamic response can be observed in method I and method II. However, the torque ripple of method II is much lower than that of method I. The reversal responses of both methods from −1500r/min to 1500r/min are presented in Fig.19. Again it is seen that the dynamic responses are similar but method II presents lower torque and flux ripples.

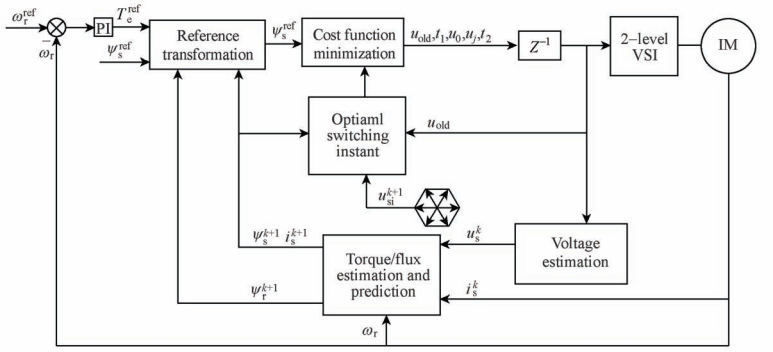

Fig.17 Control diagram of the three-vectors-based MPFC

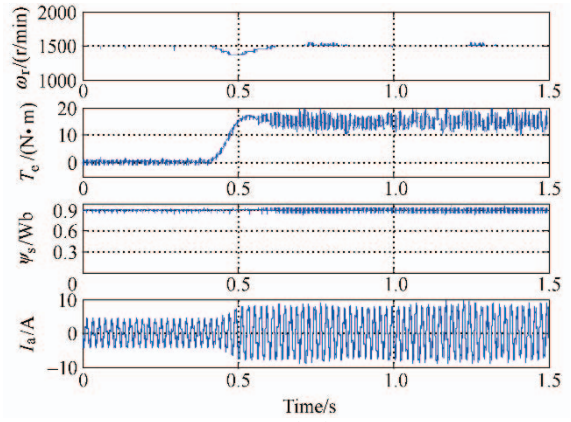

(a) Method I

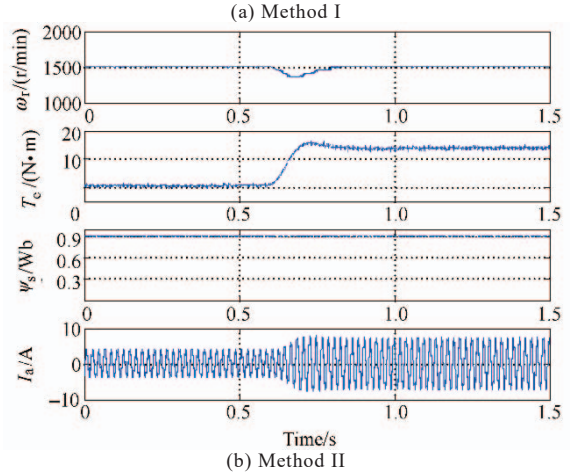

(b) Method II

Fig.18 Responses to 100% rated load disturbance for method I and method II

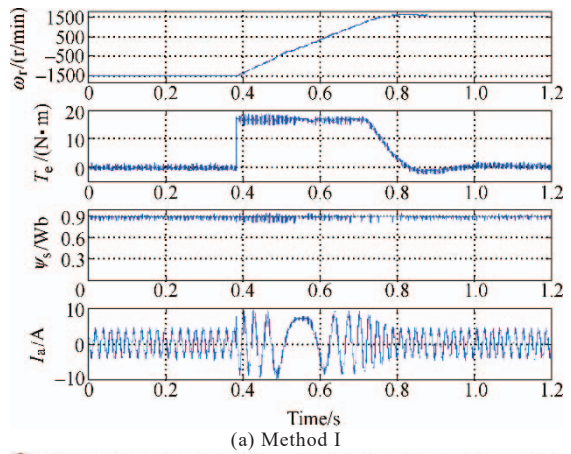

(a) Method I

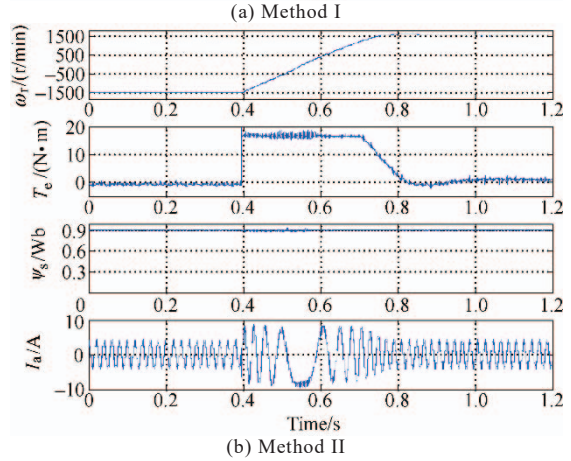

(b) Method II

Fig.19 Responses of speed reversal at 1500 r/min for method I and method II

Apart from dynamic response, steady state experiments were carried out at low speeds with a rated load disturbance, as shown in Fig.20. Both methods can work well but method II presents better steady state performance than method I in term of the torque and flux ripples.

6 Practical issues

6.1 Decreasing starting current

In MPC, the stator flux and torque are directly controlled while the stator current is not directly regulated. If the IM is started directly without any special measure on the current control, there may be a large starting current leading to over-current protection as shown in Fig.21(a). To decrease the starting current and maintain sufficient starting torque, the stator flux should first be established. The process of machine magnetization is called pre-excitation, which is achieved by the current chopping control as shown in Fig.21(b). During the process of pre-excitation, a fixed nonzero voltage vector will be selected and if the current exceeds its limitation setting, the nonzero vector will be switched to a zero vector to decrease the current. This process will not terminate until the stator flux amplitude reaches its reference value and then the IM can start safely with sufficient torque[8].

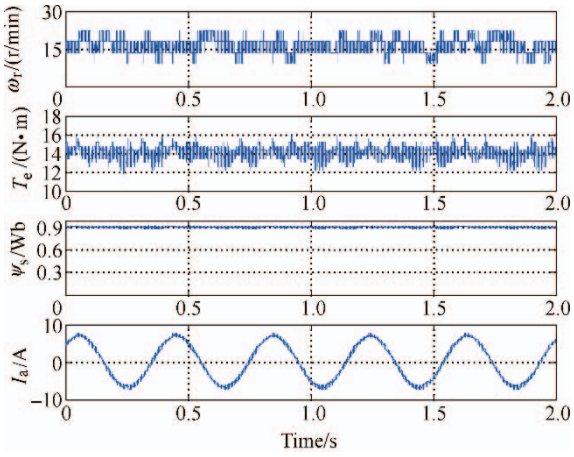

(a) Method I

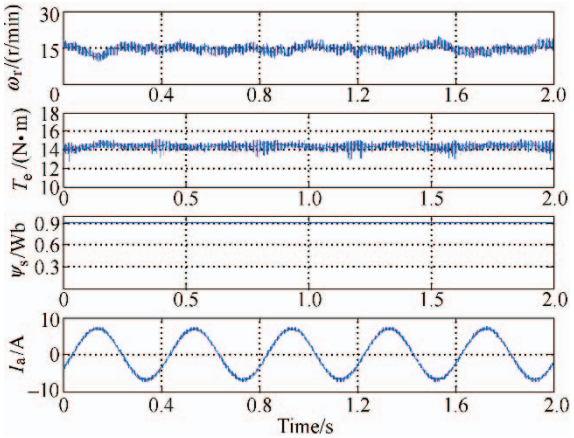

(b) Method II

Fig.20 Low speed operation of 15 rpm with rated load for method I and method II

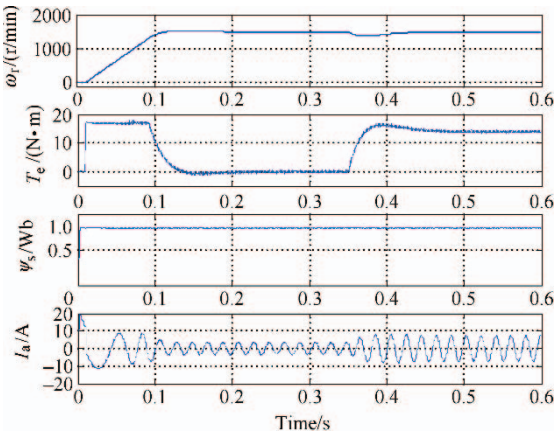

(a) Without pre-excitation

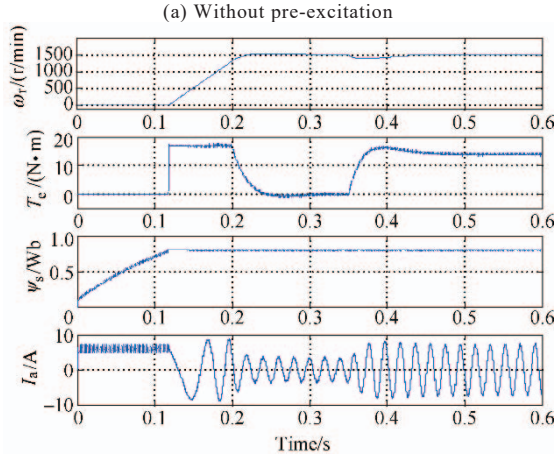

(b) Pre-excitation

Fig.21 Simulated starting responses from standstill to 1500 r/min for MPFC without pre-excitation and with pre-excitation.

6.2 Sensorless operation

Sensorless operation is preferred in many applications because of lower cost and better adaptability to hostile environments. Many schemes, such as state observer [48], model reference adaptive system [49] and Kalman filter[50], have been studied to achieve high performance closed-loop control without using a speed sensor. In this part, the combination of MPFC and an adaptive full observer[51-52] is proposed to achieve sensorless operation. To further improve the steady state performance, SVM is used to generate the final gating pulses. Experiment results prove that the proposed sensorless SVM-MPFC can achieve excellent dynamic and steady state performance over a wide speed range.

6.2.1 Deadbeat control of stator flux vector

Knowing the amplitude and angle of stator flux from(18) and (21), we can obtain the stator flux vector reference, as shown in (20). Consequently, the stator voltage vector reference can be obtained based on deadbeat control of stator flux vector, which is expressed as:

$$\boldsymbol{u}_s^{\text{ref}} = R_s \boldsymbol{i}_s^{k+1} + \frac{\boldsymbol{\psi}_s^{\text{ref}} - \boldsymbol{\psi}_s^{k+1}}{T_{sc}} \tag{22}$$

where $\boldsymbol{\psi}_s^{k+1}, \boldsymbol{i}_s^{k+1}$ can be obtained by equation (5).

6.2.2 Speed-adaptive full order

The adaptive full order observer can be constructed from the model of IM, as shown in equation (8). The control diagram of the observer is illustrated in Fig.22. From Lyapunov's theorem, the estimated speed can be obtained as [53]:

$$\frac{\mathrm{d}\hat{\omega}_r}{\mathrm{d}t} = \left(k_p + \frac{k_i}{s}\right)\left(\Delta i_{s\alpha}\hat{\psi}_{r\beta} - \Delta i_{s\beta}\hat{\psi}_{r\alpha}\right) \tag{23}$$

where $\Delta \boldsymbol{i}_s = \boldsymbol{i}_s - \hat{\boldsymbol{i}}_s$ is an error current between measurement and estimation. $\hat{\boldsymbol{\psi}}_r$ can be obtained from the equations (6) and (8).

The responses of starting from standstill to 1500 r/min and reverse to forward operation at 1500r/min for sensorless SVM-MPFC are shown in Fig.23 and Fig.24, respectively. It can be seen that the motor accelerates quickly to the reference speed with a 120% rated torque. The estimated speed follows the actual speed well during the whole process, indicating that the observer and controller work well over a wide speed range.

Apart from the dynamic response, the steady state tests at high and low speeds with rated load disturbance were carried out, as shown in Fig.25 and Fig.26. It is shown that, the estimated speed is almost identical to the actual speed and stator current wave- forms are very sinusoidal during the whole process. There are some speed fluctuations at low speed, which is mainly caused by the oscillations in the load torque. The stator current is still sinusoidal, as shown in Fig.26.

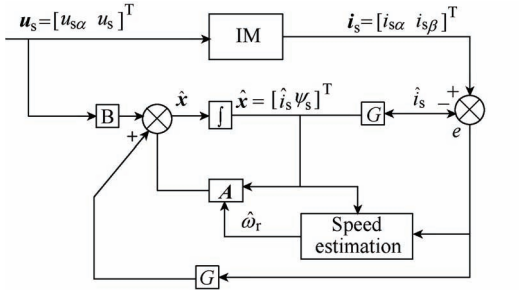

Fig.22 Control diagram of adaptive full order observer

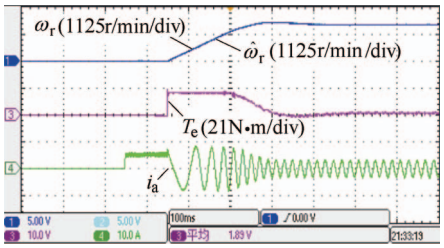

Fig.23 Starting response from standstill to 1500r/min

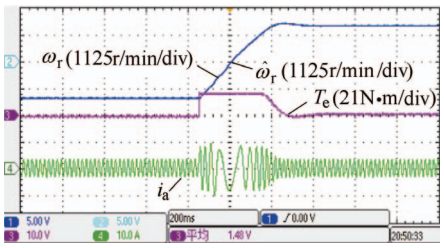

Fig.24 Reverse to forward operation at 1500r/min

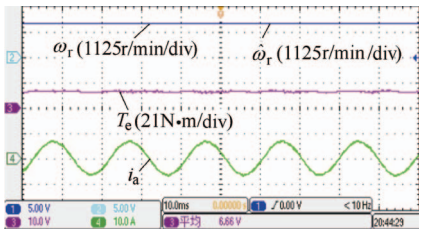

Fig.25 Steady state of 1500r/min with 100% rated

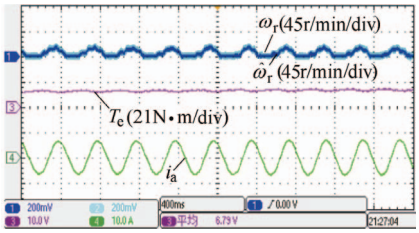

Fig.26 Steady state operation at 15r/min with 100% rated load

7 Comparison with FOC

This part introduces an improved two-vectors-based MPC[29] (MPC2) and it is compared with the well-established FOC. A detailed experimental study of both methods is presented, including steady state performance, dynamic response, and average switching frequency. Very promising results are obtained in MPC2 by providing better steady state performance and much quicker response than FOC under the condition of similar average switching frequency. The results prove that MPC2 is a powerful alternative to FOC and may find wide application in the near future.

The first voltage vector of MPC2 is selected from the six non-zero voltage vectors under the assumption that they are applied for the whole control period. After selecting the first voltage vector $\boldsymbol{u}_{1\text{opt}}$, the next step is to select the second optimal voltage vector $\boldsymbol{u}_{2\text{opt}}$ and determine the optimal duration t_{opt} of the first vector. To reduce the control complexity, the second voltage vector is selected among the vectors adjacent to $\boldsymbol{u}_{1\text{opt}}$, which produces no more than one switching jumps. The control diagram of the proposed MPC2 is shown in Fig.27.

7.1 Dynamic response

Firstly, the dynamic response of FOC and MPC2 is compared. The starting responses from standstill to 1500r/min and the reverse to forward operation for both methods are shown in Fig.28 and Fig.29, respectively.

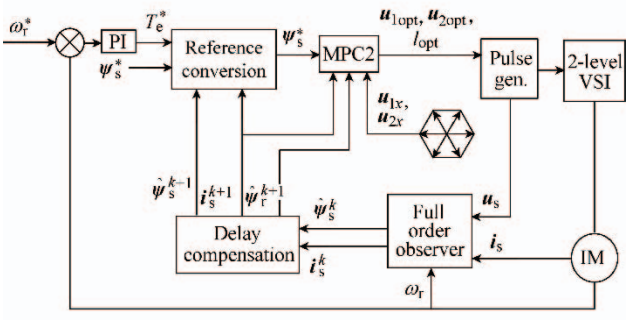

Fig.27 Control diagram of MPC2

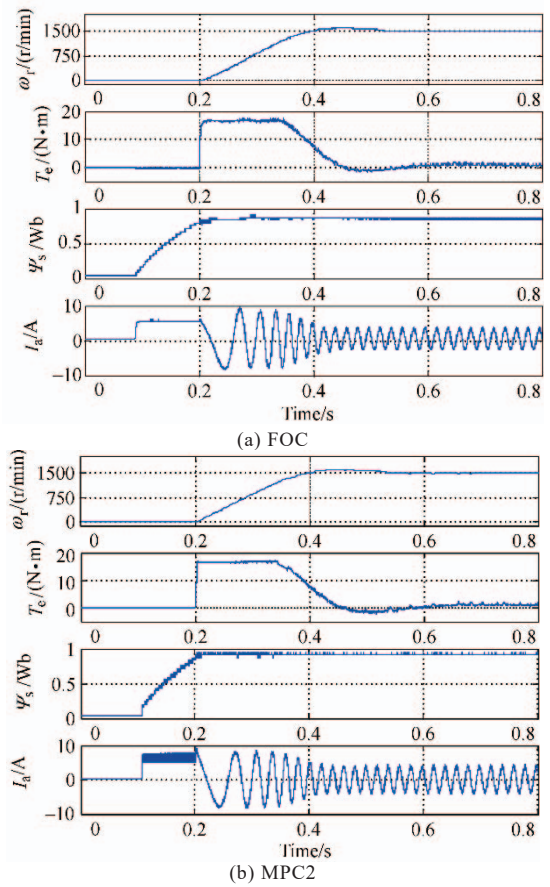

(a) FOC

(b) MPC2

Fig.28 Starting responses from standstill to 1500 r/min for FOC and MPC2

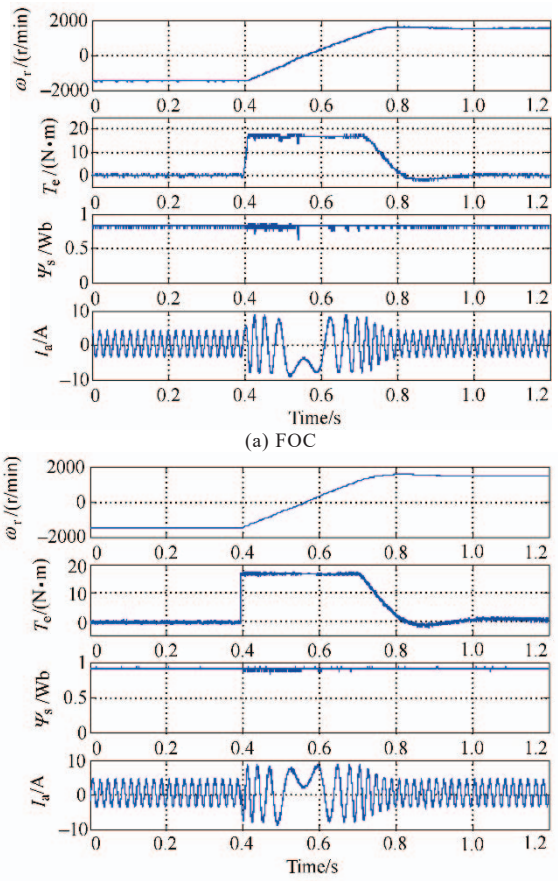

(a) FOC

(b) MPC2

Fig.29 Response of speed reversal for FOC and MPC2

It is clear that MPC2 presents better performance than FOC in terms of the torque and flux ripples.

Fig.30 illustrates the short time response of torque for both FOC and MPC2, where the torque reference changes from zero to 120% rated value suddenly at t=0.01s. The response of conventional single-vector-based MPTC[18] is also presented for the aim of comparison. It is clearly seen that the MPC2 achieves extremely quick dynamic response with rising time less than 1ms (similar to MPTC). On the contrary, it takes more than 10ms for the torque of FOC to reach the 120% rated value, which is much slower than that of MPTC and MPC2.

7.2 Steady state performance

Apart from the dynamic response comparison, Fig.31 further presents the steady state performance comparison of current THD and torque ripples for MPTC, FOC and MPC2 at various speeds. It is clearly seen that conventional MPTC presents the highest current THD and torque ripple at all speeds. The proposed MPC2 exhibits the best steady state performance in terms of current THD and torque ripple, especially in the high speed range. At low speeds below 1000r/min, the torque ripple of MPC2 is similar to that of FOC. The quantitative comparison confirms the superiority of MPC2 over FOC not only in the dynamic response, but also in steady state performance.

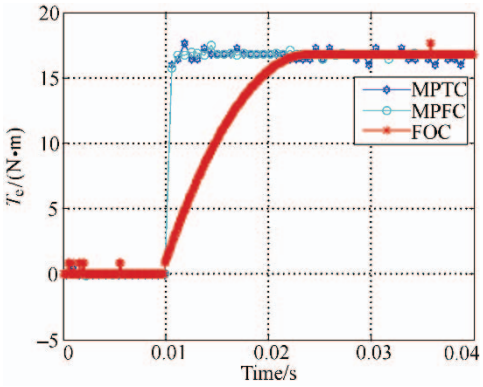

Fig.30 Comparison of short time response of torque for MPC, MPC2 and FOC

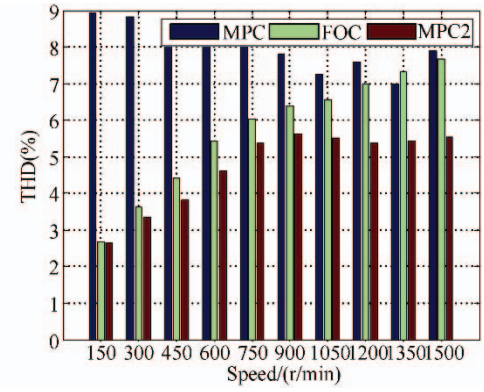

(a) Current THDs

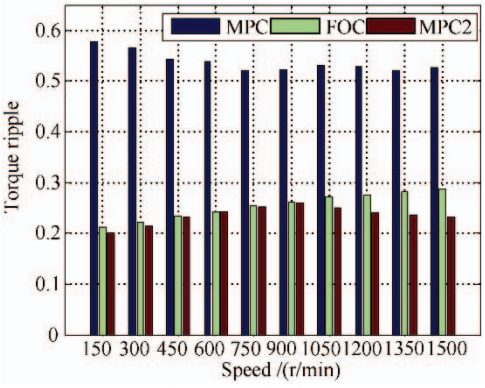

(b) Torque ripples

Fig.31 Quantitative steady state performance comparison of MPC, FOC and MPC2 at various speeds

7.3 Average switching frequency

Fig.32 shows the average switching frequency of FOC and MPC2 at various speeds. Though MPC2 presents slightly variable average switching frequency in the whole speed range, the average switching frequency of MPC2 is slightly lower than FOC.

8 Conclusion

MPC is emerging as a powerful control scheme for high performance torque control of ac motor drives. However, conventional MPC present some drawbacks which should be solved. This paper presents the state of art of MPC dealing with these problems.

The control complexity and computational burden in conventional MPC can be reduced significantly by eliminating the prediction of stator current. Only prediction of the stator flux is necessary, which is much easier to implement.

To avoid nontrivial weighting factor tuning, MPFC is developed. By investigating the inherent relationship between stator flux and torque based on IM model, a new stator flux vector reference is equivalently obtained from original references of torque and stator flux amplitude. Thus, simultaneous control of both torque and stator flux in conventional MPTC is achieved by control of stator flux vector and the weighting factor tuning is eliminated.

The steady state performance can be significantly improved by imposing two or three vectors during one control period. For two-vectors-based MPC, by relaxing the vector combinations to two arbitrary voltage vectors, Much better steady state performance verses conven-

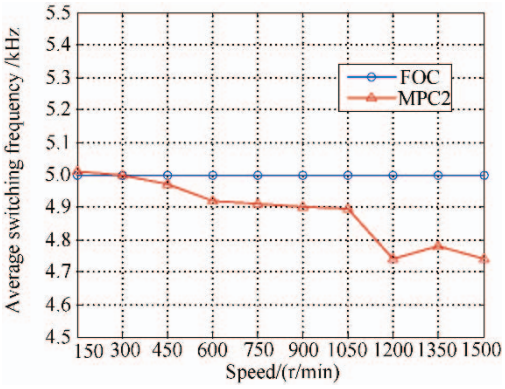

Fig.32 Comparison of average switching frequency for FOC (5 kHz sampling frequency) and MPC2 (15kHz sampling frequency)

tional MPC in terms of torque and flux ripples as well as current harmonics can be obtained at various speeds. The average switching frequency is almost constant and even lower than conventional single-vector-based MPTC at medium speeds.

For the practical operation of MPC, the per-excitation technique is very effective to reduce the starting current while providing sufficient torque. By using speed adaptive flux observer, the MPC can operate at wide speed range without speed sensors, which increases the reliability of MPC in practical applications.

Finally, a comparative experimental study of FOC and the recently two-vectors-based MPC are carried out on a two-level inverter-fed IM drive. These two methods are tested under the condition of similar average switching frequency to make a fair comparison. It is found that the two-vectors-based MPC exhibits much quicker dynamic response than that of FOC. Furthermore, the steady state performance of MPC2 in terms of current THD and torque ripple is also better than FOC, especially in the high speed range. The test results show that the two-vectors-based MPC is a powerful alternative to conventional FOC and may find wide application in the future.

References

[1] D. Casadei, F. Profumo, G. Serra, and A. Tani, "FOC and DTC: two viable schemes for induction motors torque control," *IEEE Trans. Power Electron.*, vol. 17, no. 5, pp. 779-787, Sept. 2002.

[2] S. K. Sul, *Control of Electric Machine Drive Systems*. New Jersey, USA:Wiley-IEEE Press, 2011.

[3] I. Takahashi, and T. Noguchi, "A new quick-response and high-efficiency control strategy of an induction motor," *IEEE Trans. Ind. Appl.*, vol. IA-22, no. 5, pp. 820-827, Sept. 1986.

[4] M. Depenbrock, "Direct self-control (DSC) of inverter-fed induction machine," *IEEE Trans. Power Electron*., vol. 3, no. 4, pp. 420-429,Oct. 1988.

[5] L. Zhong, M. Rahman, W. Hu, and K. Lim, "Analysis of direct torque control in permanent magnet synchronous motor drives," *IEEE Trans. Power Electron*., vol. 12, no. 3, pp. 528- 536, May 1997.

[6] T. Noguchi, H. Tomiki, S. Kondo, and I. Takahashi, "Direct power control of pwm converter without power-source voltage sensors," *IEEE Trans. Ind. Appl.*, vol. 34, no. 3, pp. 473-479, 1998.

[7] Y. Zhang, and J. Zhu, "A novel duty cycle control strategy to reduce both torque and flux ripples for dtc of permanent magnet synchronous motor drives with switching frequency reduction," *IEEE Trans. Power Electron.*, vol. 26, no. 10, pp. 3055-3067, Oct. 2011.

[8] Y. Zhang, J. Zhu, Z. Zhao, W. Xu, and D. Dorrell, "An improved direct torque control for three-level inverter-fed induction motor sensorless drive," *IEEE Trans. Power Electron*., vol. 27, no. 3, pp. 1502-1513,March 2012.

[9] G. S. Buja, and M. P. Kazmierkowski, "Direct torque control of PWM inverter-fed AC motors – a survey," *IEEE Trans. Ind. Electron.*, vol. 51, no. 4, pp. 744-757, Aug. 2004.

[10] K. K. Shyu, J. K. Lin, V. T. Pham, M. J. Yang, and T.W. Wang, "Global minimum torque ripple design for direct torque control of induction motor drives," *IEEE Trans. Ind. Electron*., vol. 57, no. 9, pp. 3148-3156, Sept.2010.

[11] J. Rodriguez, S. Bernet, B. Wu, J. Pontt, and S. Kouro, "Multilevel voltage-source-converter topologies for industrial medium-voltage drives," *IEEE Trans. Ind. Electron*., vol. 54, no. 6, pp. 2930 -2945, Dec. 2007.

[12] S. Kouro, P. Cortes, R. Vargas, U. Ammann, and J. Rodriguez, "Model predictive control—a simple and powerful method to control power converters," *IEEE Trans. Ind. Electron*., vol. 56, no. 6, pp. 1826-1838, june 2009.

[13] S. Mariethoz, A. Domahidi, and M. Morari, "High-bandwidth explicit model predictive control of electrical drives," *IEEE Trans. Ind. Appl.*, vol. 48, no. 6, pp. 1980-1992, 2012.

[14] Y. Zhang and H. Yang, "Generalized two-vector-based model-predictive torque control of induction motor drives," *IEEE Trans. Power Electron*, vol. 30, no. 7, pp. 3818-3829, 2015.

[15] Y. Zhang, and H. Yang, "Two-vector-based model predictive torque control without weighting factors for induction motor drives," *IEEE Trans. Power Electron*., vol. 31, no. 2, pp. 1381-1390, 2016.

[16] Y. Zhang, and H. Yang, "Model predictive torque control of induction motor drives with optimal duty cycle control," *IEEE Trans. Power Electron.*, vol. 29, no. 12, pp. 6593-6603, 2014.

[17] J. Holtz, "The representation of AC machine dynamics by complex signal flow graphs," *IEEE Trans. Ind. Electron.*, vol. 42, no. 3, pp.263-271, June 1995.

[18] H. Miranda, P. Cortes, J. Yuz, and J. Rodriguez, "Predictive torque control of induction machines based on state-space models," *IEEE Trans. Ind. Electron*., vol. 56, no. 6, pp. 1916- 1924, June 2009.

[19] L. J. Diao, D. nan Sun, K. Dong, L.T. Zhao, and Z.G. Liu, "Optimized design of discrete traction induction motor model at low-switching frequency," *IEEE Trans. Power Electron.*, vol. 28, no. 10, pp. 4803-4810,Oct. 2013.

[20] S. C. Chapra, and R. P. Canale, *Numerical Methods for Engineers*. New York, NY, USA: McGraw-Hill, 2010.

[21] Yongchang Zhang, and Zhengming Zhao, "Speed sensorless control for three level inverter-fed induction motors using an extended luenberger observer," in *Proc. Vehicle Power and Propulsion Conf.*, 2008, pp. 1-5.

[22] Tobias Geyer, "Model predictive direct torque control: derivation and analysis of the explicit control law," *IEEE Trans. Ind. Electron.*, vol. 49, no. 5, pp. 2146-2157, Sept 2013.

[23] T. Geyer, G. Papafotiou, and M. Morari, "Model predictive direct torque control--part I: concept, algorithm, and analysis," *IEEE Trans. Ind. Electron*., vol. 56, no. 6, pp. 1894-1905, June 2009.

[24] P. Karamanakos, P. Stolze, R. Kennel, S. Manias, and H. du Toit Mouton, "Variable switching point predictive torque control of induction machines," *IEEE Journal of Emerging and Selected Topics in Power Electronics*, vol. 2, no. 2, pp. 285-295, June 2014.

[25] J. Rodriguez, R. M. Kennel, J. R. Espinoza, M. Trincado, C. A. Silva, and C. A. Rojas, "High-performance control strategies for electrical drives: an experimental assessment," *IEEE Trans. Ind. Electron.*, vol. 59,no. 2, pp. 812-820, 2012.

[26] Y. Cho, K. B. Lee, J. H. Song, and Y. Lee, "Torque-ripple minimization and fast dynamic scheme for torque predictive control of permanent magnet synchronous motors," *IEEE Trans. Power Electron.*, vol. 30,no. 4, pp. 2182-2190, 2015.

[27] F. Wang, Z. Zhang, S. Alireza Davari, R. Fotouhi, D. Arab Khaburi, J. Rodriguez, and R. Kennel, "An encoderless predictive torque controlfor an induction machine with a revised prediction model and efosmo,"*IEEE Trans. Ind. Electron.*, vol. 61, no. 12, pp. 6635-6644, 2014.

[28] C. A. Rojas, J. Rodriguez, F. Villarroel, J. R. Espinoza, C. A. Silva, and M. Trincado, "Predictive torque and flux control without weighting factors," *IEEE Trans. Ind. Electron.*, vol. 60, no. 2, pp. 681-690, Feb. 2013.

[29] Yongchang Zhang, Bo Xia, and Haitao Yang, "Performance evaluation of an improved model predictive control with field oriented control as a benchmark," *IET Electr. Power Appl*., 2016, in press.

[30] Y. Zhang, H. Yang, and B. Xia, "Model predictive torque control of induction motor drives with reduced torque ripple," *IET Electr. Power Appl*., vol. 9, no. 9, pp. 595-604, 2015.

[31] Zhang Yongchang, and Yang Haitao. "Model predictive control for sensorless induction motor drive,"*Proceedings of the CSEE*, vol. 35, no.3, pp. 719-726, 2015. (in Chinese)

[32] Y. Zhang, H. Yang, and B. Xia, "Model predictive control of induction motor drives: flux control versus torque control," *IEEE Trans. Ind Appl*., vol. 52, pp, no. 99, pp. 1-11, 2016.

[33] J. Rodriguez, and P. Cortes, "*Predictive Control of Power Converters and Electrical Drives*," New York, NY, USA: Wiley-IEEE Press, 2012.

[34] J. Beerten, J. Verveckken, and J. Driesen, "Predictive direct torque control for flux and torque ripple reduction," *IEEE Trans. Ind. Electron*., vol. 57, no. 1, pp. 404-412, Jan. 2010.
[35] V. Ambroži˘c, G. S. Buja, and R. Menis, "Band-constrained technique for direct torque control of induction motor," *IEEE Trans. Ind. Electron.*, vol. 51, no. 4, pp. 776-784, Aug. 2004.
[36] S. A. Davari, D. A. Khaburi, and R. Kennel, "An improved FCS–MPC algorithm for an induction motor with an imposed optimized weighting factor," *IEEE Trans. Power Electron.*, vol. 27, no. 3, pp. 1540-1551, Mar.2012.
[37] Y. Zhang, and H. Yang, "Torque ripple reduction of model predictive torque control of induction motor drives," in *Proc. IEEE Energy Convers. Congr.Expo.*, 2013, pp. 1176-1183.
[38] J.-K. Kang, and S.K. Sul, "New direct torque control of induction motor for minimum torque ripple and constant switching frequency," *IEEE Trans. Ind. Appl.*, vol. 35, no. 5, pp. 1076-1082, Sept./Oct. 1999.
[39] Y. Zhang, and J. Zhu, "Direct torque control of permanent magnet synchronous motor with reduced torque ripple and commutation frequency," *IEEE Trans. Power Electron*., vol. 26, no. 1, pp. 235-248, Jan. 2011.
[40] Barrero F., Prieto J., and Levi E.,"An enhanced predictive current control method for asymmetrical six-phase motor drives", *IEEE Trans. Ind. Electron*, vol. 58, no. 8, pp. 3242-3252, 2011.
[41] Barrero F., Arahal M., and Gregor R., "One-step modulation predictive currentcontrol method for the asymmetrical dual three-phase induction machine," *IEEE Trans. Ind. Electron*., vol.56, no.6, pp. 1974-1983, 2009.
[42] Nemec M., Nedeljkovic D., and Ambrozic V.,"Predictive torque control of induction machines using immediate flux control," *IEEE Trans. Ind. Electron*., vol.54, no.4, pp. 2009-2017, 2007.
[43] Y. Zhang, H. Yang, and Z. Li, "A simple SVM-based deadbeat directtorque control of induction motor drives," in *Proc. Int. Conf. Elect. Mach. Syst*., 2013, pp.2201-2206.
[44] Y. Zhang, B. Xia, and H. Yang, "A novel three-vectors-based model predictive flux control of induction motor drives," *International Power Electronics and Motion Control Conference (IPEMC)*, 2016, pp. 367-373.
[45] Y. Zhang, and H. Yang, "Model predictive flux control of induction motor drives with switching instant optimization," *IEEE Trans. Energy Convers*, vol. 30, no. 3, pp. 1113-1122, Sept. 2015.
[46] B. Kenny, and R. Lorenz, "Stator-and rotor-flux-based deadbeat directtorque control of induction machines,"*IEEE Trans. Ind. Appl*., vol. 39,no. 4, pp. 1093-1101, July/Aug. 2003.
[47] E. Flach, R. Hoffmann, and P. Mutschler, "Direct mean torque control ofan induction motor," *in Proc. Eur. Power Electron. Drives*, 1997, vol. 3, pp. 672-677.
[48] B. Chen, T. Wang, W. Yao, K. Lee, and Z. Lu, "Speed convergence rate-based feedback gains design of adaptive full-order observer in sensorless induction motor drives," *IET Electr. Power Appl*., vol. 8, no. 1, pp. 13-22, 2014.
[49] D. Marcetic, I. Krcmar, M. Gecic, and P. Matic, "Discrete rotor flux and speed estimators for high-speed shaft-sensorless im drives," *IEEE Trans. Ind. Electron*., vol. 61, no. 6, pp. 3099-3108, June 2014.
[50] M. Habibullah, and D. D. C. Lu, "A speed-sensorless fs-ptc of induction motors using extended kalman filters," *IEEE Trans. Ind. Electron*, vol. 62, no. 11, pp. 6765-6778, Nov. 2015.
[51] Zhang Yongchang, Zhao Zhengming, Zhang Yingchao, et al. "Sensorless vector control system of induction motor fed by three-level inverter using a full order observer,"*Transactions of China Electrotechnical Society*, 2008，23(11): 34-40(in Chinese).
[52] Zhang Z, Tang R, Bai B, "Novel direct torque control based on space vector modulation with adaptive stator flux observer for induction motors" *IEEE Trans. on Magnetics*, vol. 46, no. 8, pp. 3133-3136, 2010.
[53] S. Suwankawin and S. Sangwongwanich, "Design strategy of an adaptive full-order observer for speed-sensorless induction-motor Drives-tracking performance and stabilization," IEEE *Trans. Ind. Electron.*, vol. 53, pp. 96-119, Feb. 2006.

Yongchang Zhang (M'10) received the B.S. degree from Chongqing University, China, in 2004 and the Ph.D. degree from Tsinghua University, China, in 2009, both in electrical engineering. From August 2009 to August 2011, he was a Postdoctoral Fellow at the University of Technology Sydney, Australia. He joined North China University of Technology in August 2011 as an associate professor. Currently he is a full professor and the vice director of Inverter Technologies Engineering Research Center of Beijing. He has published more than 100 technical papers in the area of motor drives, pulse width modulation and AC/DC converters. His current research interest is model predictive control for power converters and motor drives.

Bo Xia was born in 1990. He received the B.S. degree from Hunan University of Technology in 2014. He is currently working toward the Master degree in electrical engineering at North China University of Technology, Beijing, China. His research interest is model predictive control of induction motor drives.

Haitao Yang was born in 1987. He received the B.S. degree from Hefei University of Technology, China, in 2009 and the Master degree from North China University of Technology, China, in 2015, both in electrical engineering. He is currently working toward the Ph.D degree in mechanical engineering at University of Technology Sydney, Sydney, Australia. His research interest is model predictive control of AC motor drives.

Jose Rodriguez (M'81-SM'94-F'10) received the Engineer degree in electrical engineering from the Universidad Tecnica Federico Santa Maria, in Valparaiso, Chile, in 1977 and the Dr.-Ing. degree in electrical engineering from the University of Erlangen, Erlangen, Germany, in 1985. He has been with the Department of Electronics Engineering, Universidad Tecnica Federico Santa Maria, since 1977, where he was full Professor and President. Since 2015 he is the President of Universidad Andres Bello in Santiago, Chile. He has coauthored more than 400 journal and conference papers. His main research interests include multilevel inverters, new converter topologies, control of power converters, and adjustable-speed drives. He has received a number of best paper awards from IEEE. Dr. Rodriguez is member of the Chilean Academy of Engineering and Fellow of the IEEE. In 2014 he received the National Award of Applied Sciences and Technology from the Government of Chile. In 2015 he received the Eugene Mittelmann Award from IEEE.